

Observation and analysis of percolation behavior in carbon microcoils/silicone-rubber composite sheets

T. Katsuno,^{a)} X. Chen, S. Yang, and S. Motojima^{b)}

Department of Applied Chemistry, Faculty of Engineering, Gifu University, Yanagido 1-1, Gifu 501-1193, Japan

M. Homma and T. Maeno

Department of Mechanical Engineering, Keio University, Yokohama 223-8522, Japan

M. Konyo

Graduate School of Information Sciences, Tohoku University, Aoba-ku, Sendai 980-8579, Japan

(Received 4 January 2006; accepted 27 April 2006; published online 9 June 2006)

The electrical properties of carbon microcoils (CMCs)/ silicone-rubber composites were studied on the changes in the values of the electrical parameters (impedance, phase angle, resistance, and capacitance) as a function of the CMC content in the matrix, using an impedance analyzer in the frequency range from 40 to 200 kHz. Percolation paths were observed at a 3 wt % CMC content in the matrix. The properties of the composites were separated at the percolation threshold. The capacitance with a small value was dominant at CMC content less than 3 wt %, and the resistance was dominant at CMC content higher than 3 wt %. © 2006 American Institute of Physics. [DOI: 10.1063/1.2206701]

The composites of the conducting materials in an insulating host have been widely studied because of their importance in both the basic and applied sciences.¹ The electrical and thermal conductivities of the silicone-rubber used as a host with the addition of carbon nanotubes (CNTs) dramatically change depending on the concentrations and the silicone-rubber matrix.^{2–4} Moreover, the CNT/silicone-rubber composites have attracted considerable attention due to their reinforcing properties.^{5–9} The outstanding physical properties of the CNTs/silicone-rubber composite materials including these designed for structural applications are widely available for utilization in various fields such as thermal, mechanical, surface, and multifunctional properties.

Recently, it was determined that carbon microcoils (CMCs) related to the carbon family embedded in a silicone-rubber have the ability of tactile sensing based on the changes in the electrical parameters such as the resistance R , capacitance C , and inductance L while applying a load onto the sensor and can detect weak contact forces.^{10,11} The CMC tactile sensor (consisting of CMCs and silicone-rubber composites) has shown a promise for device applications. CMCs with a coil diameter of about 10–30 μm and a length of 10 μm –1 mm depending on the preparation conditions are a three-dimensional (3D)-helical-spiral structure similar for a double-helix DNA and Meissner's corpuscle in the human skin. The conductivity of a CMC is about $1 \times 10^4 \Omega^{-1} \text{cm}^{-1}$ at room temperature determined by a four-terminal resistance measurement,¹² and the CMC consists of amorphous and crystalline $\text{C}=\text{C}$ sp^2 bonding structures. The CMC/silicone-rubber composites show unique tactile sensing properties; however, we do not know why CMC tactile sensors have different values of the electrical signals by changing the sensor sizes and CMC contents in the matrix and produce a few weak electrical signals. In this letter, we focused on the im-

pedance Z , phase angle θ , resistance R , and capacitance C of the CMC/silicone-rubber composites without an applied load in order to investigate the electrical properties within the micro-order domains depending on the CMC content in the matrix using the same size sheets analyzed by an impedance analyzer.

The CMCs were synthesized by the thermal chemical vapor deposition (CVD) method at the temperature of 770 °C catalyzed by Ni powder, which was placed on a graphite substrate placed within a vertical quartz tube.¹³ The CMCs with a diameter of about 20 μm and a coil length of 90–150 μm were used in this study, which produced as-grown CMCs with a diameter of 1 μm as shown in Fig. 1(b). The silicone-rubber (KE-103) was supplied by Shin-Etsu Chemical Co., Ltd., as a host matrix due to its good softness and elasticity. When the CMCs were blended with a silicone-rubber resin, small bubbles appeared in the CMCs/silicone-rubber composites. The bubbles were removed by a 30 min application, before the mixture was hardened to form the composite sheets. The CMC sensor elements had the size of $10 \times 10 \times 3 \text{mm}^3$ and they were prepared with the different CMC contents of 0, 1, 2, 3, 4, 5, 7 and 10 wt % in the matrix. Thin sensor sheets with a thickness of about 100 μm were cut from the sensor element and observed using an optical microscope (OLYMPUS, BX51). Figure 1(a) shows a micro-

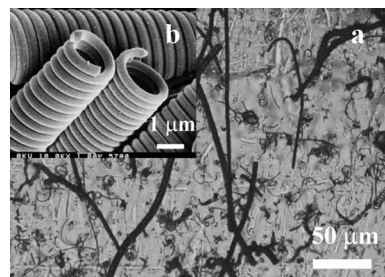


FIG. 1. (a) Optical microscopic image of CMCs/silicone-rubber composite. (b) SEM image of as-grown CMCs, showing the coils used with no gap.

^{a)}Electronic mail: katsuno@apchem.gifu-u.ac.jp

^{b)}Electronic mail: motojima@apchem.gifu-u.ac.jp

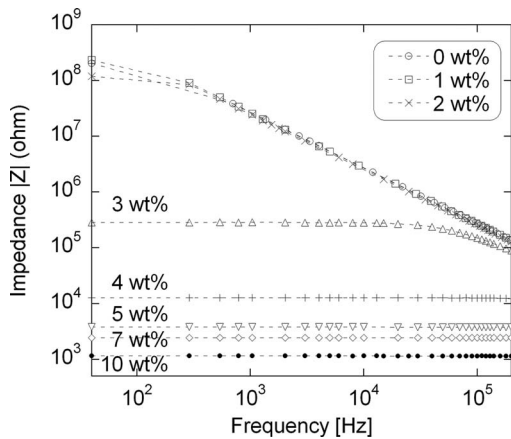


FIG. 2. The dependence of impedance Z on frequency as a function of the CMC content for the CMC/silicone-rubber composite sheets.

scopic photograph of these thin sensor sheets (CMCs 2 wt %) embedded in the silicone-rubber. The light was irradiated from the back side, and all of the microstructure through the entire thickness of the sheet was observed. Small carbon micro-nanofibers with short lengths were also observed. Figure 1(b) shows the representative as-grown CMCs obtained by scanning electron microscopy (Topcon, ABT-150F).

In order to measure the electrical parameters such as impedance Z and the phase angle θ of the CMC/silicone-rubber composite sensor elements, an impedance analyzer (Agilent Technology, 4294A) was used in the frequency range from 40 to 200 kHz with the voltage of 0.5 V. The sample was placed on two electrodes whose length, width, and separation were 10, 3, and 2 mm, respectively. Impedance vector consists of a real part (resistance R) and an imaginary part (reactance X). Therefore, the impedance Z and phase angle θ can be expressed as follows:

$$Z = R + jX, \quad \theta = \tan^{-1}\left(\frac{X}{R}\right). \quad (1)$$

The above parameters were used to discuss the electrical properties of the CMCs/silicone-rubber composites.

Figure 2 shows the dependence of the impedance Z on frequency as a function of the CMC content. The spectra with the CMC contents from 0 to 2 wt % are almost the same and decrease from 10^8 to $5 \times 10^5 \Omega$ as the frequency increases from 40 to 200 kHz, indicating a strong dependence on frequency. However, the impedance Z suddenly decreased at 3 wt % as compared to the content of 0–2 wt % and gradually decreased with the increasing CMC content, showing almost no dependence on frequency over the entire range (horizontal spectra). The dependences of the phase angle θ on frequency as a function of the CMC content are shown in Fig. 3. For the CMC contents of 1–2 wt %, the values of the phase angle are nearly -90° , indicating that the capacitive property is similar to the pure silicone-rubber over the entire frequency range. Having the same tendency in Fig. 2, the phase angle suddenly changed from 0° to -70° at the CMC content of 3 wt % as the frequency ranged from 40 to 200 kHz and becomes nearly flat (0°) with the increasing CMC content, showing a direct link between the impedance Z and phase angle θ . The phase angle is almost 0° at the CMC content above 3 wt % which means that the CMC/

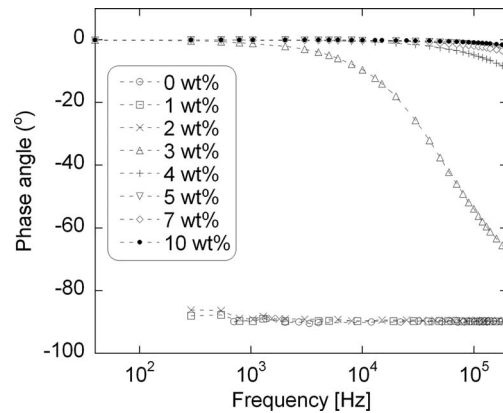


FIG. 3. The dependence of the phase angle θ on frequency as a function of the CMC content for the CMC/silicone-rubber composite sheets.

silicone-rubber composites consist of a large resistance R and a small reactance X .

The dependences of Z and the phase angle θ on CMC contents at the selected frequency of 200 kHz obtained from Figs. 2 and 3 are shown in Fig. 4. Z was almost constant up to 2 wt % but suddenly decreased at 3 wt %, while θ was also almost the same below 2 wt % but dramatically increased at 3 wt %. These results indicated that the CMCs started percolation paths in the micro-order domains at the CMC content of 3 wt %, and the electrical properties of the CMC/silicone-rubber composites are separated at 3 wt %. The changes in the low CMC concentrations (<3 %) show no significant influence on the electrical properties, which are deduced to seldom pass electrons through the matrix. Furthermore, Z and θ were saturated above 4 wt % with the values of 10^3 – $10^4 \Omega$ and 0° , respectively. According to the phase angle θ the CMC/silicone-rubber composites would consist of two components, the resistance R and capacitance C because θ is between -90° and 0° . The inductance L component produced from the CMCs is negligible in this study because the current pass as through the cylinder along the coil pitches¹² due to these types of CMCs with no gap as shown in Fig. 1. Besides, the CMC/silicone-rubber composites are better for use in a parallel connection with the components of R_p and C_p simulated by an equivalent circuit in the frequency range from 40 to 200 kHz, as compared with the serial connection (will be presented in another paper). In this case $1/Z = 1/(R + jX) = Y = G + jB$, where Y represents the

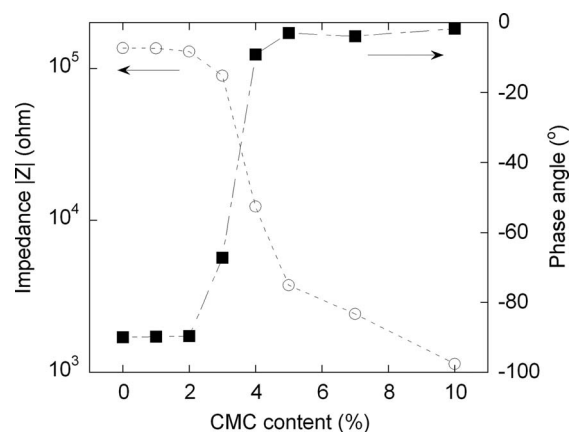


FIG. 4. The dependence of the impedance Z and phase angle θ on the CMC content at the selected frequency of 200 kHz obtained from Figs. 2 and 3.

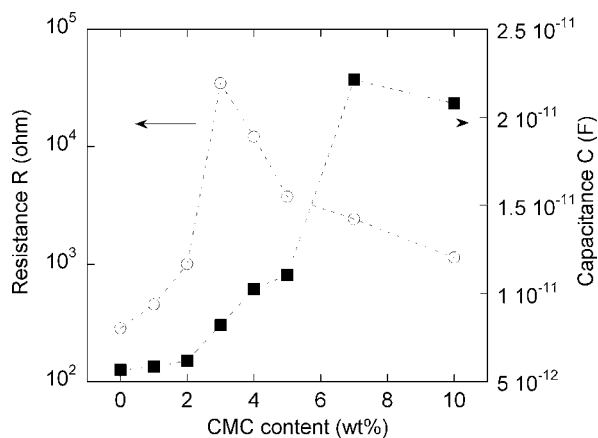


FIG. 5. The dependence of the resistance R_p and capacitance C_p on the CMC content at the selected frequency of 200 kHz. R_p and C_p were calculated from $R=1/G$ and $B=2\pi fC_p$, respectively.

admittance, G the conductance, and B the susceptance. Therefore, the capacitance C_p is determined from $B=2\pi fC_p$, where f is the frequency.

Figure 5 shows the dependence of the resistance R_p and capacitance C_p on the CMC content at the selected frequency of 200 kHz. R_p increased with the increasing CMC content up to 3 wt % with the percolation threshold value and then decreased with increasing CMC content. However, C increased with the increasing CMC content over the entire range. The CMCs/silicone-rubber composites below the percolation threshold have properties similar to pure silicone-rubber, showing that the capacitance C is very small, which indicates that $|X|=1/B=1/2\pi fC$ is extremely high as compared to the resistance R [$|X|\gg|R|$] as shown in Eq. (1)]. Thus the phase angle is -90° . Almost all the CMCs do not touch each other due to the increase in the CMC numbers below the percolation threshold. To start the percolation paths at 3 wt %, the CMCs touch each other in the micro-order domains; therefore, R decreased with the increasing CMC content. Some CMCs without touching each other can produce a capacity in the silicone-rubber matrix due to the closed CMCs with the increasing CMC content. The increased capacitance C means that $|X|=1/B=1/2\pi fC$ significantly de-

creased with the increasing CMC content. Thus the phase angle shows 0° [$|X|\ll|R|$] as shown in Eq. (1)].

In conclusion, we reported the electrical properties of the micro-order domains in the CMCs/silicone-rubber composite sheets due to the changes in the values of the electrical parameters (impedance Z , phase angle θ , resistance R and capacitance C) as a function of the CMC content in the matrix. Percolation paths were observed at a 3 wt % CMC content. The CMCs/silicone-rubber composites indicated that the dominant capacitive (low capacitance C indicated extremely high $|X|=1/2\pi fC\gg|R|$, showing the value of -90°) and resistive properties (high C indicated low $|X|=1/2\pi fC\ll|R|$, showing the value of 0°) were separated at the percolation threshold. Although R decreased above the percolation threshold by touching some CMCs, the capacitance C increases due to the increasing capacity in the silicone-rubber matrix by the closed CMCs touching each other.

This work was supported by the Gifu-Ogaki Robotics Medical Cluster.

- ¹B. E. Kilbride, J. N. Coleman, J. Fraysse, P. Fournet, M. Cadek, A. Drury, S. Hutzler, S. Roth, and W. J. Blau, *J. Appl. Phys.* **92**, 4024 (2002).
- ²X.-L. Xie, Y.-W. Mai, and X.-P. Zhou, *Mater. Sci. Eng., R.* **49**, 89 (2005).
- ³R. H. Baughman, A. A. Zakhidov, and W. A. de Heer, *Science* **297**, 787 (2002).
- ⁴H. Yanagi, E. Sawada, A. Manivannan, and L. A. Nagahara, *Appl. Phys. Lett.* **78**, 1355 (2001).
- ⁵E. S. Choi, J. S. Brooks, D. L. Eaton, M. S. Al-Haik, M. Y. Hussaini, H. Garmestani, D. Li, and K. Dahmen, *J. Appl. Phys.* **94**, 6034 (2003).
- ⁶B. Vigolo, A. Pénicaud, C. Coulon, C. Sauder, R. Paillet, C. Journet, P. Bernier, and P. Poulin, *Science* **290**, 1331 (2000).
- ⁷H. D. Wagner, O. Lourie, Y. Feldman, and R. Tenne, *Appl. Phys. Lett.* **72**, 188 (1998).
- ⁸L. Jin, C. Bower, and O. Zhou, *Appl. Phys. Lett.* **73**, 1197 (1998).
- ⁹O. Lourie, D. M. Cox, and H. D. Wagner, *Phys. Rev. Lett.* **81**, 1638 (1998).
- ¹⁰X. Chen, S. Yang, M. Hasegawa, K. Kawabe, and S. Motojima, *Appl. Phys. Lett.* **87**, 054101 (2005).
- ¹¹M. Homma, M. Konyo, T. Maeno, H. Morita, and S. Motojima (unpublished).
- ¹²Y. Kajihara, T. Hihara, K. Sumiyama, and S. Motojima, *Jpn. J. Appl. Phys., Part 1* **44**, 6867 (2005).
- ¹³X. Chen and S. Motojima, *J. Mater. Sci.* **34**, 5519 (1999).